JOURNAL OF VIROLOGY, Dec. 2008, p. 12164–12171 Vol. 82, No. 24
0022-538X/08/$08.00+0 doi:10.1128/JVI.01158-08

Human T-Cell Lymphotropic Virus Type 1 Nucleocapsid Protein-Induced Structural Changes in Transactivation Response DNA Hairpin Measured by Single-Molecule Fluorescence Resonance Energy Transfer▽

Qusai Darugar,[1] Hannah Kim,[1] Robert J. Gorelick,[2] and Christy Landes[1]*

Department of Chemistry, University of Houston, Houston, Texas 77204-5003,[1] and AIDS and Cancer Virus Program, SAIC-Frederick, Inc., NCI-Frederick, Frederick, Maryland 21702-1201[2]

Received 3 June 2008/Accepted 22 September 2008

Time-resolved single-molecule fluorescence spectroscopy was used to study the human T-cell lymphotropic virus type 1 (HTLV-1) nucleocapsid protein (NC) chaperone activity compared to that of the human immunodeficiency virus type 1 (HIV-1) NC protein. HTLV-1 NC contains two zinc fingers, each having a CCHC binding motif similar to HIV-1 NC. HIV-1 NC is required for recognition and packaging of the viral RNA and is also a nucleic acid chaperone protein that facilitates nucleic acid restructuring during reverse transcription. Because of similarities in structures between the two retroviruses, we have used single-molecule fluorescence energy transfer to investigate the chaperoning activity of the HTLV-1 NC protein. The results indicate that the HTLV-1 NC protein induces structural changes by opening the transactivation response (TAR) DNA hairpin to an even greater extent than HIV-1 NC. However, unlike HIV-1 NC, HTLV-1 NC does not chaperone the strand-transfer reaction involving TAR DNA. These results suggest that, despite its effective destabilization capability, HTLV-1 NC is not as effective at overall chaperone function as is its HIV-1 counterpart.

Human T-cell lymphotropic virus type 1 (HTLV-1) shares many common features with human immunodeficiency virus type 1 (HIV-1). HTLV-1 is of interest because infection with this virus can lead to adult T-cell leukemia, as well as certain types of demyelinating diseases, such as tropical spastic paraparesis (1, 6). The HIV-1 retrovirus has been widely studied, and it is known that both of these viruses contain many different structural and functional proteins (9, 10, 12, 18, 19, 22, 29), including the nucleocapsid proteins (NC), which are common in other retroviruses as well (11). In HIV-1, NC proteins play a critical role in chaperoning the strand transfer reactions during the reverse transcription process (27, 36, 45, 48). The HIV-1 NC protein is characterized by two zinc fingers that have a highly conserved CCHC binding motif as shown in Fig. 1a. Although the first and second zinc fingers of the NC proteins are similar, their biological activities are different. Despite their differing biological activities, both zinc fingers are necessary for viral replication (16, 20, 21).

Guo et al. have shown that zinc ion coordination plays an important role in the efficient minus- and plus-strand transfer steps of reverse transcription (23). Specifically, the zinc fingers destabilize base pairing of the nucleic acid, hence destabilizing the transactivation response RNA (TAR-RNA) and TAR-DNA (4). Furthermore, it has been reported that nucleic acid chaperone activity is not supported by changing the amino acid residues surrounding the zinc-binding CCHC residues, either by duplicating and/or exchanging the zinc fingers in the two positions, as each zinc finger performs a specific function during the strand transfer process (24). Two independent functions of HIV-1 NC during reverse transcription include nucleic acid aggregation (15, 34) and duplex destabilization (3–5, 23, 49, 50, 53) associated with the N-terminal basic amino acid domain and the zinc fingers, respectively.

The HTLV-1 NC protein, like the HIV-1 NC, contains two zinc finger motifs, as shown in Fig. 1b, but the overall amino acid sequence of the HIV-1 protein is basic, whereas HTLV-1 NC is a neutral protein. HTLV-1 NC is 85 amino acids (aa) in length containing a basic N-terminal region and a negatively charged C-terminal tail (43). A major difference between the HTLV-1 and HIV-1 NC proteins is the 35-aa extension on the C-terminal end of HTLV-1 NC that is quite acidic. The NC proteins from HIV-1 and the closely related deltaretrovirus, bovine leukemia virus (BLV), have an extension of only 6 aa at their C termini (12).

All retroviruses undergo minus-strand transfer in which part of the minus-strand strong stop DNA must anneal to the viral RNA. This involves, to a greater or lesser extent depending on the specific retrovirus, both destabilization and annealing events. The strand transfer process and the region of TAR-DNA/RNA involved are well characterized for HIV. Thus, using TAR is a useful benchmark to study how other retroviral proteins function during viral replication. As mentioned before, one of the most important functions of the HIV-1 NC protein is to chaperone the annealing of HIV-1 TAR-RNA to the complementary sequence (TAR-DNA) in minus-strand strong-stop DNA. Unlike the HIV-1 NC protein chaperone activity in reverse transcription (10, 14, 17, 20, 21, 23, 24, 30, 37, 38, 54, 55), little is known about the activity of the NC protein in HTLV-1 and other retroviruses during this process. Recently, retroviral specific differences in NC's nucleic acid binding, aggregation, and overall chaperone function have been reported (47). By comparing structural and chemical properties between HIV-1 and HTLV-1 NC proteins, the effects of these proteins on binding to the HIV-1 TAR-DNA hairpin can

* Corresponding author. Mailing address: Department of Chemistry, University of Houston, 136 Fleming, Houston, TX 77204-5003. Phone: (713) 743-3288. Fax: (713) 743-2709. E-mail: cflandes@uh.edu.
▽ Published ahead of print on 1 October 2008.

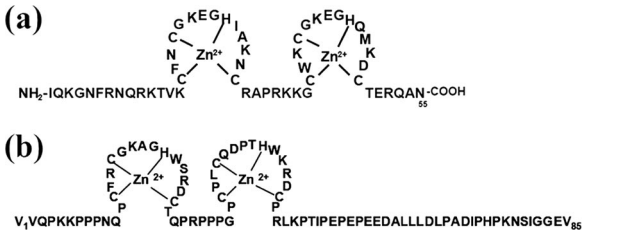

FIG. 1. Structures of HIV-1 NC protein (a) and HTLV-1 NC protein (b).

provide a greater insight into critical mechanisms and roles played by these proteins in reverse transcription. Ultimately, understanding how the NC proteins affect viral infection can be useful in targeting drugs for disease prevention and control. The present study compares HIV-1 and HTLV-1 NC protein-chaperoned opening of the TAR-DNA hairpin and the reaction with zipper DNA (cDNA for the nucleation occurring at the 3′/5′ termini of the TAR-DNA opened at bulge L2 (37) using time-resolved single-molecule spectroscopy to identify the underlying mechanism behind NC protein activity.

Fluorescence resonance energy transfer (FRET) is a useful technique for measuring average configurations. Because of the dynamic heterogeneity intrinsic to biomolecules, a more useful technique for measuring dynamics is single-molecule FRET (SMFRET). SMFRET is a powerful tool for obtaining information about complex processes at a molecular level (38, 40, 41). Specifically, SMFRET has been used successfully to observe structural fluctuations in biomolecules (25, 42, 52, 56). Because one measures these dynamic changes one molecule at a time, it is possible to eliminate the averaging that occurs when all molecules are measured concurrently, as in traditional ensemble FRET. Time-resolved single-molecule spectroscopy has been used in previous studies to measure the nucleic acid conformational dynamics (9, 10, 35, 37, 38, 54, 55). Nucleic acid conformation changes in the presence of proteins have been observed using SMFRET (7). By monitoring the real-time fluorescence signals from a donor-acceptor (D/A) fluorescent dye pair, it is possible to extract information about the dynamics of TAR-DNA hairpin opening and closing, in the presence or absence of NC proteins. FRET efficiency can be used as a tool to measure the extent of structural changes as a function of distance between the dyes when the NC proteins interact with the D/A TAR-DNA hairpin. Furthermore, fluctuations in the FRET efficiency reveal kinetic information from these systems in solution.

SMFRET analysis using the HIV-1 system performed by Cosa et al. showed that the NC protein destabilizes the secondary structure in the 3′/5′-terminal loop regions of the initially closed TAR-DNA hairpin (9) (the closed form is the C form shown in Fig. 7a below). Liu et al. used SMFRET to study important intermediates in the NC protein chaperoned minus-strand transfer step in HIV-1 reverse transcription (37, 38). They showed that in addition to destabilizing the hydrogen bonds of the TAR-DNA hairpin up to bulge L2, leading to the Y form structure, the HIV-1 NC protein assists the complementary zipper DNA (Fig. 2) to anneal to the Y form structure of TAR-DNA. The interaction between D/TAR-DNA and A/zipper DNA was monitored by observing the time resolved

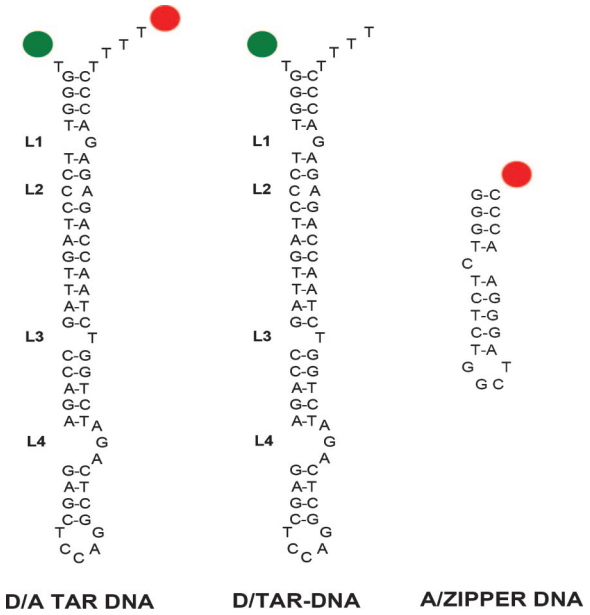

FIG. 2. Structures of TAR-DNA and zipper DNA used in the SMFRET studies.

FRET between the donor and acceptor dyes as the NC protein chaperones the annealing of the DNA strands. The FRET data revealed the importance of HIV-1 NC protein in unzipping the TAR-DNA hairpin and reannealing the zipper DNA to the melted region similar to the process occurring during minus-strand transfer during reverse transcription.

We show here that the HTLV-1 NC protein also disrupts the HIV-1 TAR-DNA hairpin bonds. In addition, we tested the ability of HTLV-1 NC protein to chaperone the annealing of two DNA strands. Both the FRET trajectory study and the reactions with complementary zipper DNA gave us insights into the extent to which the TAR-DNA hairpin opens up in the presence of HTLV-1 NC protein and whether it assists in annealing complementary nucleic acids.

MATERIALS AND METHODS

Sample preparation. Purified Cy3 (donor)- and Cy5 (acceptor)-labeled biotinylated TAR-DNA (D/A TAR-DNA) was purchased from TriLink Biotechnologies (San Diego, CA). HTLV-1 NCp15 protein was prepared as follows: the gene encoding HTLV-1 NCp15 was PCR amplified from a full-length HTLV-1 proviral plasmid pCS-HTLV-1 (13) (a generous gift from David Derse, NCI-Frederick) and cloned into pET32a (Novagen, a brand of EMD Biosciences, Inc., Madison, WI) to generate the plasmid pDR2559 that expresses HTLV NCp15 as a thioredoxin fusion with a TEV protease cleavage site (ENLYFQ) (31, 32). The HIV-1 NCp7 expression construct was prepared as described previously (8). Once the HTLV-1 and HIV-1 NC fusion proteins were expressed and cleaved with TEV protease or enterokinase, respectively, the full-length HTLV-1 NCp15 and HIV-1 NCp7 (NL4-3; GenBank accession no. AF324493) were prepared and purified essentially as described previously (8, 23). Figures 1 and 2 show the sequences and structures of the NC proteins and the biotinylated DNA used in these experiments, respectively. D/A TAR-DNA was immobilized on the coverslip by using biotinylated polyethylene glycol (biotin-PEG-NHS-5000; NOF Corp., Japan).

Before PEG immobilization, plasma-cleaned coverslips were first treated with Vectabond-acetone 1% (wt/vol) solution (Vector Laboratories, Burlingame, CA) for 5 min and then rinsed with molecular biology-grade water (HyClone; VWR) and dried with an N_2 stream.

Vectabond-treated coverslips were covered with a silicon template with an oval opening. The exposed area was incubated with 25% m-PEG-SPA-5000 (Sigma)

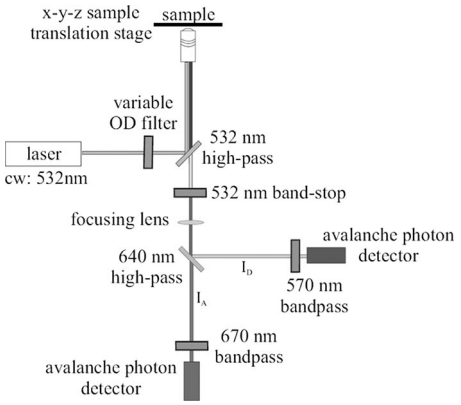

FIG. 3. Laboratory-built single-molecule spectroscopy/polarization microscope.

and 0.25% biotin-PEG-NHS-5000 in 0.1 M sodium bicarbonate for 3 h. The silicon template was removed, and the excess PEG solution was rinsed with molecular biology-grade water and dried with N_2. A reaction chamber was constructed over the incubated area using flow inlet and outlet ports (Upchurch Scientific) and predrilled polycarbonate films with customized adhesive seals (Grace Bio). This reaction chamber made it possible to flow solutions over the treated surface. The chamber was filled with a streptavidin solution—0.2 mg/ml in HEPES buffer (25 mM HEPES, 40 mM NaCl [pH 7.3])—and incubated in the dark for 10 min. Meanwhile, DNA solution was prepared using 10 μl of 10 nM D/A TAR-DNA in 25 mM HEPES buffer. The TAR-DNA solution was flowed into the chamber after the streptavidin and was incubated for 20 min. The excess TAR-DNA solution was then rinsed with 25 mM HEPES buffer.

During FRET analysis, a syringe pump was used to continuously flow an oxygen scavenger solution through the sample chamber to minimize the effect of rapid photobleaching of the acceptor and donor dyes. The oxygen scavenger solution was prepared by using 3% (wt/vol) β-D-(+)-glucose (Sigma), 0.1 mg of glucose oxidase/ml, 0.02 mg of catalase (Roche Applied Science)/ml, 2 mM Mg^{2+}, HEPES buffer, and saturated Trolox solution (6-hydroxy-2,5,7,8-tetramethylchroman-2-carboxylic acid; Fluka). The HIV-1 NC and HTLV-1 NC protein concentration flowed through the sample chamber were maintained at 0.44 μM in all experiments. This concentration was chosen because it is high enough to be considered saturating, quantified by the degree of fluctuations and strand transfer, and low enough that protein/nucleic acid aggregation effects are not observed (10). Detailed studies of concentration effects on these properties at lower concentrations have been reported previously (10, 38).

The reaction between the D/TAR-DNA and the A/zipper DNA was performed by first immobilizing D/TAR-DNA onto the coverslip as described

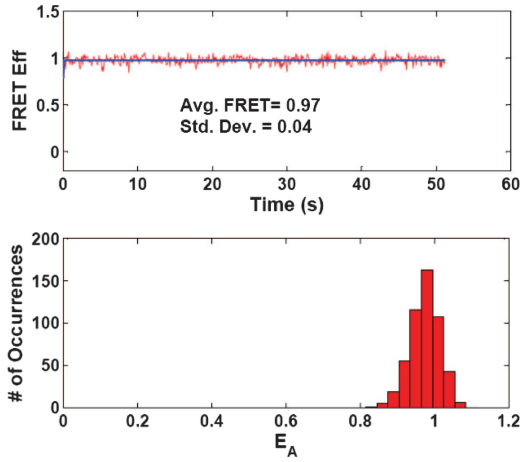

FIG. 4. FRET trajectory (top) and the corresponding FRET histogram (bottom) for single closed-structure TAR-DNA hairpin.

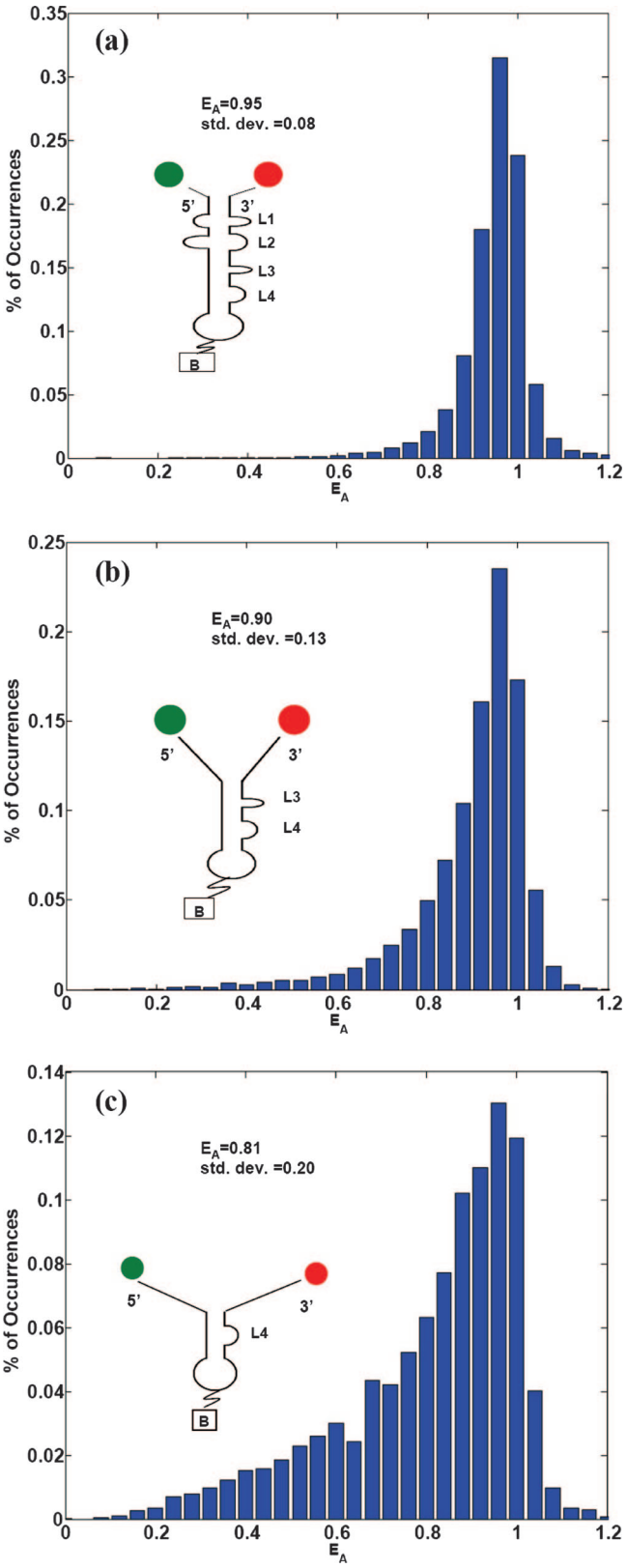

FIG. 5. Ensemble FRET histogram of D/A TAR-DNA with no NC proteins (a), in the presence of HIV-1 NC proteins (b), and in the presence of HTLV-1 NC proteins (c). For all experiments, the Mg^{2+} and NC protein concentrations were maintained at 2 mM and 0.44 μM, respectively.

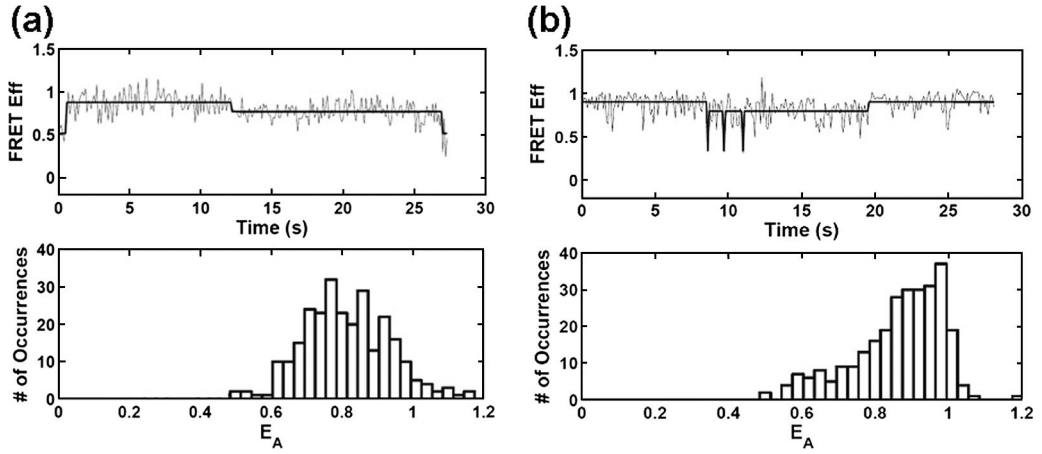

FIG. 6. (a) FRET trajectory (top) and the corresponding FRET histogram (bottom) of individual D/A TAR-DNA hairpin in the presence of HTLV-1 NC. (b) FRET trajectory of a different TAR-DNA hairpin in the presence of HTLV-1 NC. Both trajectories show highly dynamic fluctuations between the closed and open states in the presence of HTLV-1 NC compared to fluctuations seen in the presence of HIV-1 NC.

above. A series of three syringe pumps were used to systematically flow a 20 nM solution of A/zipper DNA, NC protein, and oxygen scavenger solutions as needed for the reactions.

Instrumentation/SMFRET setup. Figure 3 shows a schematic of our instrumentation. A 532-nm solid state laser (Verdi; Coherent) was used for sample excitation. The light was expanded to overfill the back aperture of a Fluar ×100 1.3 NA oil immersion microscope objective lens (Carl Zeiss, GmbH) (28). This resulted in a $1/e^2$ beam radius and height of ~230 nm and ~1 μm, respectively. The power laser light at the sample was maintained at about 310 nW/cm^2 in order to provide adequate signal to noise while minimizing instantaneous photobleaching of the dyes. Fluorescence was collected and refocused by the same objective (33) and separated from the excitation light by using a dichroic mirror (z532rdc; Chroma Technology). Additional emission filters were used to improve the signal-to-noise ratio (NHPF-532.0; Kaiser Optical; and ET585, Chroma Technology). The signal was refocused and passed through a second dichroic mirror to separate the donor and acceptor emission. The donor and acceptor fluorescence signals were collected with two avalanche photodiodes (SPCM-AQR-15; Perkin-Elmer). A closed-loop xyz piezo stage (P-517.3CL; Physik Instrumente) with 100-by-100-by-20-μm travel range and a 1-nm specificity was used to position the sample (SPM 1000; RHK Technology). Transistor-transistor logic output from the detectors was augmented and split via a fan-out buffer (PRL-414B; Pulse Instruments) to two separate computer boards: one for single photon counting trajectories (PMS-400-A; Boston Electronics Corp.) and the other for two-dimensional imaging (RHK Technology). The intensity trajectories were acquired at a 1-ms resolution and later binned up to 10 ms to improve the signal-to-noise ratio. The fluorescence signals were corrected for background noise (before binning) and donor/emission cross talk between channels (9). All of the data were analyzed with software written in house using MATLAB (R2006a).

The corrected fluorescence signal trajectories were used directly to calculate the FRET efficiency, E_A, using the following equation (37, 55):

$$E_{A(t)} = I_{A(t)}/[I_{A(t)} + I_{D(t)}] \quad (1)$$

where I_D and I_A are the background-corrected donor and acceptor signals, respectively.

Data acquisition. To obtain SMFRET trajectories for individual DNA molecules, a 10-μm-by-10-μm area of the sample was scanned to spatially locate 15 to 20 molecules. The RHK controller was then used to precisely position the piezo stage to focus the laser excitation light on a single molecule. The molecule was excited with the laser light, and the avalanche photodiodes and photon counter board collected time-resolved donor (I_D) and acceptor (I_A) fluorescence signals until photobleaching of the dye occurred. The corresponding FRET trajectory was calculated by using equation 1. Figure 4 shows an SMFRET trajectory and the corresponding FRET histogram of a TAR-DNA hairpin. This process was repeated to obtain FRET trajectories from at least 40 molecules for each experiment.

To observe the reaction between the D/TAR-DNA and A/zipper DNA, a solution of oxygen scavenger was flowed through the sample chamber for 10 min, after which a 30-μm-by-30-μm image was scanned to locate molecules. This area was then continuously scanned after the flow of A/zipper DNA solution and the NC proteins was started. The real-time scanning of the reaction area revealed the chaperoning effects of NC proteins on DNA through the time-resolved fluorescence signals from the molecules as they were recorded on the donor and acceptor channels.

RESULTS AND DISCUSSION

FRET trajectories and histogram. Single-molecule fluorescence trajectories record the dynamic conformational fluctuations of the D/A TAR-DNA hairpin in the absence or presence of either the HIV-1 or HTLV-1 NC proteins. Equation 1 is used to calculate the FRET efficiency time trace for each individual molecule. Figure 5 shows the ensemble FRET histograms for D/A TAR-DNA under three different experimental conditions: TAR-DNA only (panel a), TAR-DNA in the presence of HIV-1 NC protein (panel b), and TAR-DNA in the presence of HTLV-1 NC protein (panel c). The average FRET efficiency for D/A TAR-DNA only was calculated to be 0.95, which indicates that the hairpin is in a closed state (C form) in the absence of NC proteins (see Fig. 7a).

As shown previously (9, 10, 37, 38, 54, 55) and in Fig. 5b, the presence of HIV-1 NC proteins reduces the FRET efficiency from 0.95 to 0.90, implying that the TAR-DNA is in a partially opened "Y" state in the presence of HIV-1 NC protein, reducing the efficiency of energy transfer between the dyes. It is important to note that the average FRET value calculated reflects an equilibrium between closed and open states. Cosa et al. first showed (9) that the structural change that occurs in the presence of HIV-1 NC protein that gives rise to the Y-form structure corresponds to disruptions in the secondary structure up to bulge L2 as shown in Fig. 7b. A total of 6 to 7 bp break to open up the TAR-DNA hairpin to form this Y structure.

SMFRET trajectories and the corresponding histograms from individual TAR-DNA hairpin in the presence of HTLV-1 are shown in Fig. 6. State-to-state transitions identified from hidden-Markov modeled trajectories (39) clearly exhibit fluctuations between the closed and multiple open states (Fig. 6a). In contrast, a FRET trajectory from a single TAR-DNA molecule (see Fig. 4) shows no such fluctuations and in the presence of HIV-1 NC (9,

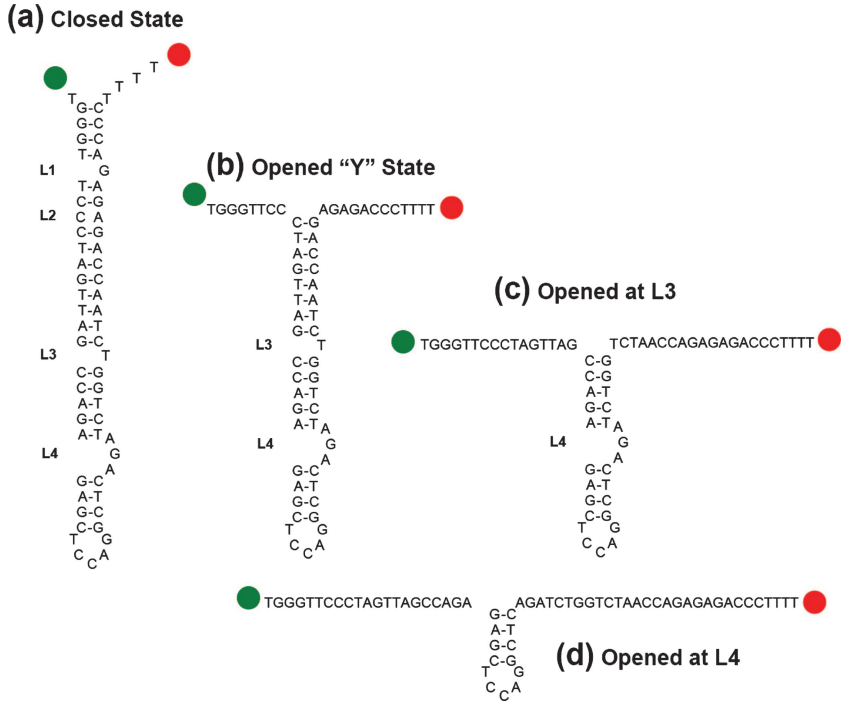

FIG. 7. Structures showing four different states of D/A TAR-DNA. Structures: completely closed "C" structure (a); structure opened at bulge L2, "Y" form (b); structures opened at bulge L3 (c) and opened at bulge L4 (d), both referred to as Y′.

37) shows fewer fluctuations and fewer open states. The observed ensemble FRET efficiency in the presence of HTLV-1 NC decreases to ~0.81, indicating that the TAR-DNA hairpin opens significantly further in the presence of HTLV-1 NC protein than it does in the presence of HIV-1 NC protein. This lower energy transfer indicates that the hairpin structure is opened up at a bulge lower than L1 and L2, i.e., to L3 or L4 (Fig. 7c and d).

Transition lifetime analyses. The ensemble FRET trajectories for TAR-DNA in the presence NC protein were further analyzed to extract information about the transitions from closed to open states by performing a transition lifetime analysis. Transition lifetime analysis examines the distributions of lifetimes of a particular state and can provide kinetic information by fitting reactant state lifetimes to an exponential decay. FRET values between 0.93 and 1.0 were set to indicate the closed state (C-form) conformation of the TAR-DNA hairpin. FRET values from 0.75 to 0.93 were set to indicate the open Y form, and values from 0.00 to 0.75 were attributed to the more widely open state Y′, achieved for TAR-DNA in the presence of HTLV-1 NC protein. The FRET for each of these three states covers a range

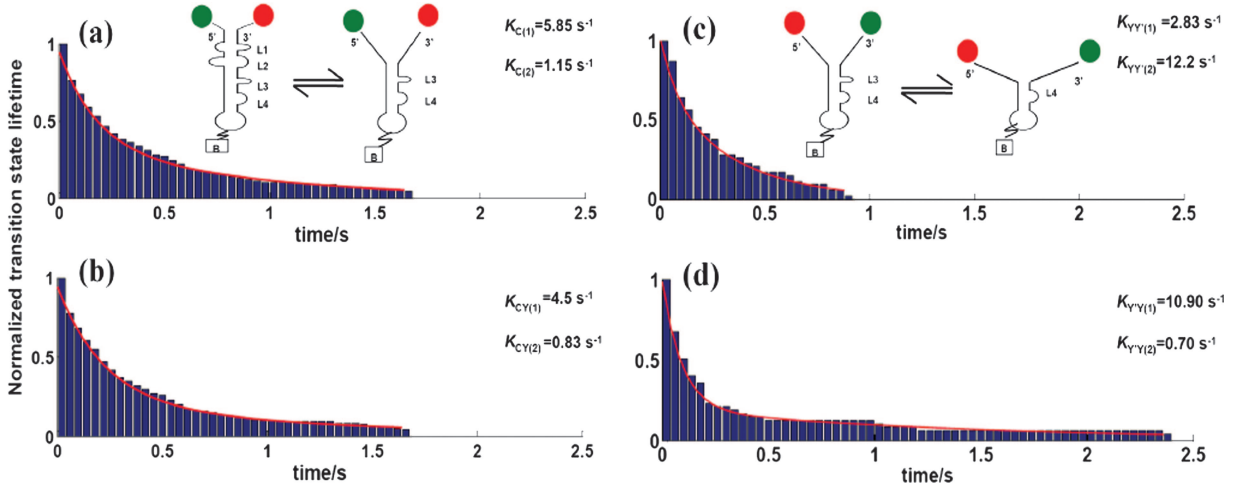

FIG. 8. Transition lifetime analysis between the closed (C) state and opened states transitions. Panel a gave a total of 258 transitions from the C state (TAR-DNA/HIV-1 NC), of which ~200 go to the Y-form state as shown in panel b. In the presence of HTLV-1 NC protein, the transition is mostly between state Y and an even more open state Y′, as shown in panels c and d, respectively.

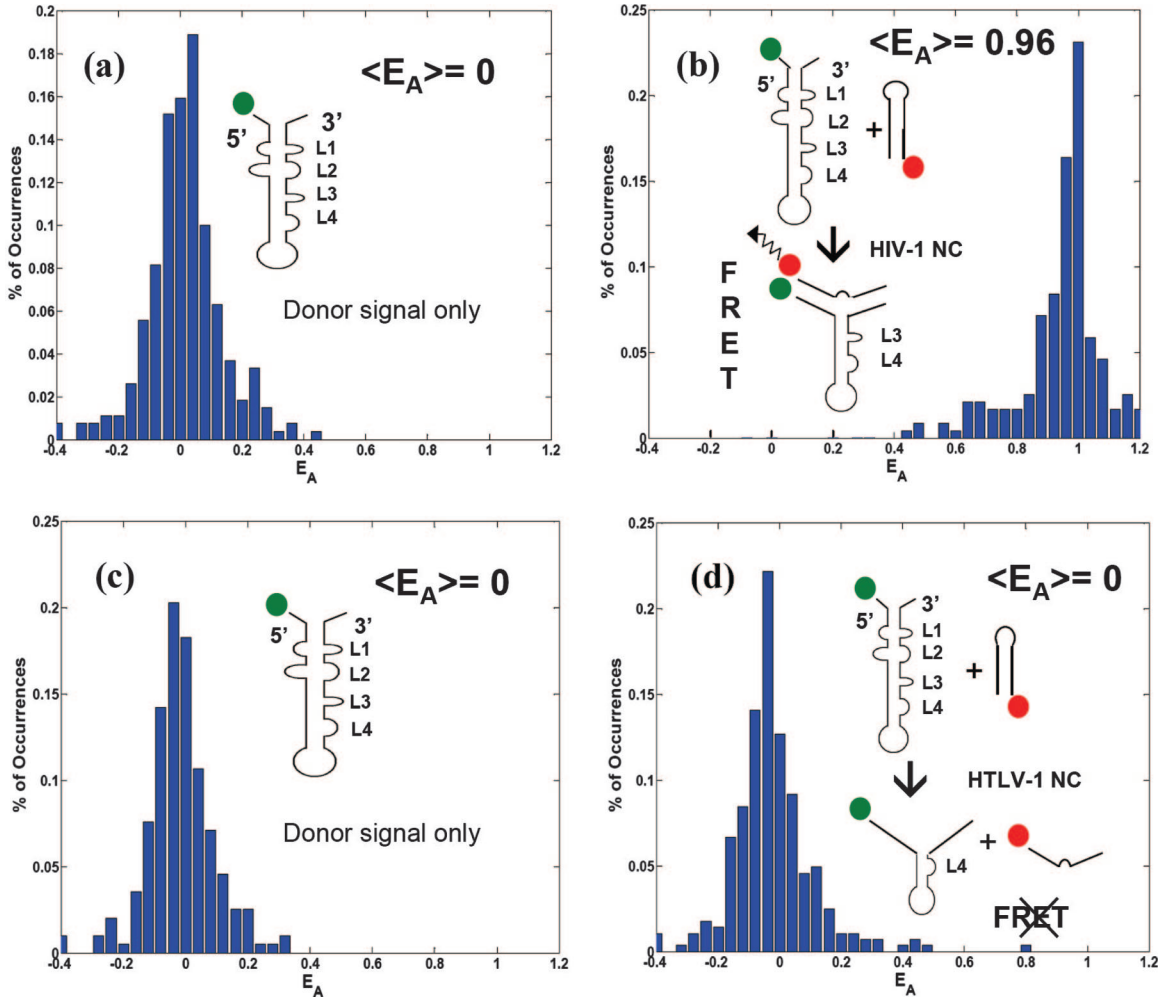

FIG. 9. Experimental ensemble FRET histograms. Panels a and c show FRET histograms calculated before adding A/zipper DNA or NC proteins, i.e., only donor signal is observed, and hence the average FRET efficiency is zero. (b) In the presence of HIV-NC protein and A/zipper DNA, the emergence of acceptor signal is seen, and the calculated average FRET efficiency is about 1. (d) In the presence of HTLV-1 NC protein and A/zipper DNA, no acceptor signal was observed with a calculated average FRET efficiency of zero.

of values to account for the open/closed equilibrium fluctuations that occur in each state.

The calculated average FRET is truly the equilibrium value between the closed and open states and does not reflect the actual FRET value for any given state. The TAR-DNA histogram in the presence of HIV-1 NC protein can be deconvoluted into two distributions that show the appropriate FRET values for the transition lifetime analysis. In the presence of HIV-1 NC protein, a total of 258 transitions from the C form were identified (Fig. 8a). Within the FRET range discussed above, a total of 198 transitions (~80% of transition C) (Fig. 8b) were identified in the Y form. This implies that in the presence of HIV-1 NC the TAR-DNA hairpin fluctuates between the closed and the partially open Y form.

The transition lifetime analysis for TAR-DNA in the presence of HTLV-1 NC protein shows a shift in the C-form transition and the hairpin fluctuates between the partially open Y form and the even more open (Y′) state (>90% transitions from state Y to state Y′) identified previously (Fig. 8c and d). It is likely that that HTLV-1 NC protein-induced structural change in the TAR-DNA hairpin is too fast to resolve the C-form state. In addition, the fit of the transition lifetime curves for all transition show bi-exponential decay. The transition rates in the presence of HIV-1 NC, i.e., from state C (K_C) and from state C to state Y (K_{CY}) and similarly the respective rates in the presence of HTLV-1 NC, as shown in Fig. 8, indicate that the transitions in the presence of NC proteins are not a simple two-state equilibrium but a rather more complicated and dynamic transition between the states, as suggested by Cosa et al. (10) as well.

Reaction between TAR-DNA and zipper DNA. Continuing the comparison between HIV-1 and HTLV-1 NC protein, the second part of the experiment measures the annealing portion of the nucleic acid chaperoning effect of the NC proteins for reactions between D/TAR-DNA and Y form A/zipper DNA (55). The reaction between the D/TAR-DNA and the A/zipper DNA in the presence of HIV-1 NC protein shows the emergence of the acceptor fluorescence signal as the reaction proceeds (Fig. 8).

Figures 9a and b show the ensemble FRET histograms be-

fore and after addition of the HIV-1 NC protein and the A/zipper DNA, respectively. The initial FRET efficiency is zero when no acceptor dye is present in the system. As HIV-1 NC and A/Zipper solutions flow through, signal from the acceptor dye is observed and the FRET efficiency changes from ~0 to ~1. The presence of HIV-1 NC protein clearly chaperones melting and annealing reactions between the two DNA strands. However, when D/TAR-DNA is reacted with A/zipper DNA and HTLV-1 NC protein, the annealing reaction was not chaperoned. This can be observed in that the FRET efficiency before and after the presence of A/zipper and HTLV-1 NC protein remained at zero as shown in Fig. 9c and d, respectively.

It is known that the opening and annealing of the TAR-DNA hairpin is critical for the minus-strand transfer process in reverse transcription (9, 10, 24, 30, 37, 38, 54, 55). Both HTLV-1 and HIV-1 NC proteins induce secondary structure fluctuations in the hairpin as seen above. Even though the zipper DNA used in our experiments is complementary to the Y-form structure rather than the Y′ structure, if HTLV-1 NC protein were efficient at reannealing the two strands, the zipper DNA should partially anneal at the 5′ region of the TAR-DNA as shown by Cosa et al. (9) using different mutant DNAs in the presence of HIV-1 NC protein. Since we do not observe any acceptor signal in the presence of HTLV-1 NC protein, it is clear that even though HTLV-1 NC protein is effective in opening the TAR-DNA hairpin, it is not effective in assisting the zipper/TAR-DNA annealing reaction.

Most retroviral NC proteins are highly charged cationic proteins. High-affinity cationic binding of these proteins to nucleic acid is predominantly electrostatic, which can lead to the formation of protein-induced nucleic acid aggregation (2, 26). However, HTLV-1 NC is neutral at physiological pH. The inability of HTLV-1 NC to aggregate nucleic acid is consistent with the electrostatic model since a high density of acidic residues are at the C terminus, whereas the majority of the basic residues are at the zinc fingers and the N terminus (44, 46). Wang et al. have shown that in BLV both NC and matrix domains are important for viral packaging (51). HTLV-1 NC, which is closely related to BLV NC, may also require an additional protein to chaperone the strand transfer reaction. Future efforts will examine this relationship in detail.

Conclusion. We used SMFRET spectroscopy to report for the first time the implications of HTLV-1 NC protein nucleic acid chaperone function on the TAR-DNA hairpin. We found that the HTLV-1 NC protein is effective in opening the TAR-DNA hairpin, even more so than the HIV-1 NC protein. This implies that the structures and basic compositions of the NC proteins play an important role in inducing structural changes in TAR-DNA since both HTLV-1 NC protein and HIV-1 NC protein have two zinc finger motifs that are highly capable of destabilizing base pairs. In addition, unlike HIV-1 NC protein, HTLV-1 NC protein is not effective at reannealing the zipper DNA and TAR-DNA. The difference in the C-terminal chain and the overall charge of the NC proteins is likely affecting the strand transfer activity, and therefore we suggest that both the zinc fingers and the termini of NC proteins are important in the strand transfer process.

ACKNOWLEDGMENTS

We thank Karin Musier-Forsyth, Kristen Stewart-Maynard, and Ioulia Rouzina for helpful discussions. We thank Cathy V. Hixson and Donald G. Johnson of the AIDS Vaccine Program, SAIC-Frederick, Inc., and NCI-Frederick, for their assistance in the preparation of the recombinant proteins used in this study.

We thank the University of Houston and the Texas Center for Superconductivity for new faculty startup funds. This study has been funded in whole or in part with federal funds from the National Cancer Institute, National Institutes of Health, under contract N01-CO-12400.

The content of this publication does not necessarily reflect the views or policies of the Department of Health and Human Services, nor does mention of trade names, commercial products, or organizations imply endorsement by the U.S. Government.

REFERENCES

1. **Ahmed, Y. F., S. M. Hanly, M. H. Malim, B. R. Cullen, and W. C. Greene.** 1990. Structure-function analyses of the HTLV-1 Rex and HIV-1 Rev. RNA response elements: insights into the mechanism of Rex and Rev. action. Genes Dev. **4:**1014–1022.
2. **Arscott, P. G., C. Ma, J. R. Wenner, and V. A. Bloomfield.** 1995. DNA condensation by cobalt hexamine(III) in alcohol-water mixtures: dielectric constant and other solvent effects. Biopolymers **36:**345–364.
3. **Azoulay, J., J.-P. Clamme, J.-L. Darlix, B. P. Roques, and Y. Mely.** 2003. Destabilization of the HIV-1 complementary sequence of TAR by the nucleocapsid protein through activation of conformational fluctuations. J. Mol. Biol. **326:**691–700.
4. **Beltz, H., J. Azoulay, S. Bernacchi, J.-P. Clamme, D. Ficheux, B. Roques, J.-L. Darlix, and Y. Mely.** 2003. Impact of the terminal bulges of HIV-1 cTAR DNA on its stability and the destabilizing activity of the nucleocapsid protein NCp7. J. Mol. Biol. **328:**95–108.
5. **Bernacchi, S., S. Stoylov, E. Piemont, D. Ficheux, B. P. Roques, J. L. Darlix, and Y. Mely.** 2002. HIV-1 nucleocapsid protein activates transient melting of least stable parts of the secondary structure of TAR and its complementary sequence. J. Mol. Biol. **317:**385–399.
6. **Bertola, F., C. Manigand, P. Picard, M. Belghazi, and G. Precigoux.** 2000. Human T-lymphotrophic virus type I nucleocapsid protein NCp15: structural study and stability of the N-terminal zinc-finger. Biochem. J. **352:**293–300.
7. **Bokinsky, G., L. G. Nivon, S. Liu, G. Chai, M. Hong, K. M. Weeks, and X. Zhuang.** 2006. Two distinct binding modes of a protein cofactor with its target RNA. J. Mol. Biol. **361:**771–784.
8. **Carteau, S., R. J. Gorelick, and F. D. Bushman.** 1999. Coupled integration of human immunodeficiency virus type 1 cDNA ends by purified integrase in vitro: stimulation by the viral nucleocapsid protein. J. Virol. **73:**6670–6679.
9. **Cosa, G., E. J. Harbron, Y. Zeng, H.-W. Liu, D. B. O'Connor, C. Eta-Hosokawa, K. Musier-Forsyth, and P. F. Barbara.** 2004. Secondary structure and secondary structure dynamics of DNA hairpins complexed with HIV-1 NC protein. Biophys. J. **87:**2759–2767.
10. **Cosa, G., Y. Zeng, H.-W. Liu, C. F. Landes, D. E. Makarov, K. Musier-Forsyth, and P. F. Barbara.** 2006. Evidence for non-two-state kinetics in the nucleocapsid protein chaperoned opening of DNA hairpins. J. Phys. Chem. B **110:**2419–2426.
11. **Darlix, J.-L., M. Lapadat-Tapolsky, H. de Rocquigny, and B. P. Roques.** 1995. First glimpses at structure-function relationships of the nucleocapsid protein of retroviruses. J. Mol. Biol. **254:**523–537.
12. **Derse, D., S. A. Hill, G. Princler, P. Lloyd, and G. Heidecker.** 2007. Resistance of human T-cell leukemia virus type 1 to APOBEC3G restriction is mediated by elements in nucleocapsid. Proc. Natl. Acad. Sci. USA **104:**2915–2920.
13. **Derse, D., J. Mikovits, M. Polianova, B. K. Felber, and F. Ruscetti.** 1995. Virions released from cells transfected with a molecular clone of human T-cell leukemia virus type I give rise to primary and secondary infections of T cells. J. Virol. **69:**1907–1912.
14. **Dettenhofer, M., S. Cen, B. A. Carlson, L. Kleiman, and X. F. Yu.** 2000. Association of human immunodeficiency virus type 1 Vif with RNA and its role in reverse transcription. J. Virol. **74:**8938–8945.
15. **Dib-Hajj, F., R. Khan, and D. P. Giedroc.** 1993. Retroviral nucleocapsid proteins possess potent nucleic acid strand renaturation activity. Protein Sci. **2:**231–243.
16. **Dorfman, T., J. Luban, S. P. Goff, W. A. Haseltine, and H. G. Gottlinger.** 1993. Mapping of functionally important residues of a cysteine-histidine box in the human immunodeficiency virus type 1 nucleocapsid protein. J. Virol. **67:**6159–6169.
17. **Driscoll, M. D., and S. H. Hughes.** 2000. Human immunodeficiency virus type 1 nucleocapsid protein can prevent self-priming of minus-strand strong stop DNA by promoting the annealing of short oligonucleotides to hairpin sequences. J. Virol. **74:**8785–8792.
18. **Frankel, A. D., and J. A. T. Young.** 1998. HIV-1: fifteen proteins and an RNA. Annu. Rev. Biochem. **67:**1–25.

19. **Freed, E. O.** 1998. HIV-1 gag proteins: diverse functions in the virus life cycle. Virology **251:**1–15.
20. **Gorelick, R. J., D. J. Chabot, A. Rein, L. E. Henderson, and L. O. Arthur.** 1993. The two zinc fingers in the human immunodeficiency virus type 1 nucleocapsid protein are not functionally equivalent. J. Virol. **67:**4027–4036.
21. **Gorelick, R. J., T. D. Gagliardi, W. J. Bosche, T. A. Wiltrout, L. V. Coren, D. J. Chabot, J. D. Lifson, L. E. Henderson, and L. O. Arthur.** 1999. Strict conservation of the retroviral nucleocapsid protein zinc finger is strongly influenced by its role in viral infection processes: characterization of HIV-1 particles containing mutant nucleocapsid zinc-coordinating sequences. Virology **256:**92–104.
22. **Grossman, W. J., J. T. Kimata, F. Wong, M. Zutter, T. J. Ley, and L. Ratner.** 1995. Development of leukemia in mice transgenic for the tax gene of human T-cell leukemia virus type I. Proc. Natl. Acad. Sci. USA **92:**1057–1061.
23. **Guo, J., T. Wu, J. Anderson, B. F. Kane, D. G. Johnson, R. J. Gorelick, L. E. Henderson, and J. G. Levin.** 2000. Zinc finger structures in the human immunodeficiency virus type 1 nucleocapsid protein facilitate efficient minus- and plus-strand transfer. J. Virol. **74:**8980–8988.
24. **Guo, J., T. Wu, B. F. Kane, D. G. Johnson, L. E. Henderson, R. J. Gorelick, and J. G. Levin.** 2002. Subtle alterations of the native zinc finger structures have dramatic effects on the nucleic acid chaperone activity of human immunodeficiency virus type 1 nucleocapsid protein. J. Virol. **76:**4370–4378.
25. **Ha, T.** 2001. Single-molecule fluorescence resonance energy transfer. Methods **25:**78–86.
26. **Heilman-Miller, S. L., J. Pan, D. Thirumalai, and S. A. Woodson.** 2001. Role of counterion condensation in folding of the *Tetrahymena* ribozyme II. Counterion dependence of folding kinetics. J. Mol. Biol. **309:**57–68.
27. **Herschlag, D.** 1995. RNA chaperones and the RNA folding problem. J. Biol. Chem. **270:**20871–20874.
28. **Hess, W.** 2002. Focal volume optics and experimental artifacts in FCS. Biophys. J. **83:**2300–2317.
29. **Hinuma, Y., K. Nagata, M. Hanaoka, M. Nakai, T. Matsumoto, K.-I. Kinoshita, S. Shirakawa, and I. Miyoshi.** 1981. Adult T-cell leukemia: antigen in an ATL cell line and detection of antibodies to the antigen in human sera. Proc. Natl. Acad. Sci. USA **78:**6476–6480.
30. **Johnson, P. E., R. B. Turner, Z. R. Wu, L. Hairston, J. Guo, J. G. Levin, and M. F. Summers.** 2000. A mechanism for plus-strand transfer enhancement by the HIV-1 nucleocapsid protein during reverse transcription. Biochem. **39:**9084–9091.
31. **Kapust, R. B., J. Toezser, J. D. Fox, D. E. Anderson, S. Cherry, T. D. Copeland, and D. S. Waugh.** 2001. Tobacco etch virus protease: mechanism of autolysis and rational design of stable mutants with wild-type catalytic proficiency. Protein Eng. **14:**993–1000.
32. **Kapust, R. B., J. Tozser, T. D. Copeland, and D. S. Waugh.** 2002. The P1′ specificity of tobacco etch virus protease. Biochem. Biophys. Res. Commun. **294:**949–955.
33. **Koppel, D. E., D. Axelrod, J. Schlessinger, E. L. Elson, and W. W. Webb.** 1976. Dynamics of fluorescence marker concentration as a probe of mobility. Biophys. J. **16:**1315–1329.
34. **Krishnamoorthy, G., B. Roques, J.-L. Darlix, and Y. Mely.** 2003. DNA condensation by the nucleocapsid protein of HIV-1: a mechanism ensuring DNA protection. Nucleic Acids Res. **31:**5425–5432.
35. **Landes, C. F., Y. Zeng, H. W. Liu, K. Musier-Forsyth, and P. F. Barbara.** 2007. Single-Molecule study of the Inhibition of HIV-1 transactivation response region DNA/DNA annealing by argininamide. J. Am. Chem. Soc. **129:**10181–10188.
36. **Levin, J. G., J. Guo, I. Rouzina, and K. Musier-Forsyth.** 2005. Nucleic acid chaperone activity of HIV-1 nucleocapsid protein: critical role in reverse transcription and molecular mechanism. Prog. Nucleic Acids Res. Mol. Biol. **80:**217–286.
37. **Liu, H.-W., G. Cosa, C. F. Landes, Y. Zeng, B. J. Kovaleski, D. G. Mullen, G. Barany, K. Musier-Forsyth, and P. F. Barbara.** 2005. Single-molecule FRET studies of important intermediates in the nucleocapsid-protein-chaperoned minus-strand transfer step in HIV-1 reverse transcription. Biophys. J. **89:**3470–3479.
38. **Liu, H.-W., Y. Zeng, C. F. Landes, Y. J. Kim, Y. Zhu, X. Ma, M.-N. Vo, K. Musier-Forsyth, and P. F. Barbara.** 2007. Insights on the role of nucleic acid/protein interactions in chaperoned nucleic acid rearrangements of HIV-1 reverse transcription. Proc. Natl. Acad. Sci. USA **104:**5261–5267.
39. **McKinney, S. A., C. Joo, and T. Ha.** 2006. Analysis of single-molecule FRET trajectories using hidden Markov modeling. Biophys. J. **91:**1941–1951.
40. **Moerner, W. E.** 1995. Optical spectroscopy of individual molecules trapped in solids. AIP Conf. Proc. **323:**467–486.
41. **Moerner, W. E., and L. Kador.** 1989. Optical detection and spectroscopy of single molecules in a solid. Phys. Rev. Lett. **62:**2535.
42. **Moerner, W. E., and M. Orrit.** 1999. Illuminating single molecules in condensed matter. Science **283:**1670–1676.
43. **Morcock, D. R., B. P. Kane, and J. R. Casas-Finet.** 2000. Fluorescence and nucleic acid binding properties of the human T-cell leukemia virus-type 1 nucleocapsid protein. Biochim. Biophys. Acta Protein Struct. Mol. Enzymol. **1481:**381–394.
44. **Nguyen, T. T., I. Rouzina, and B. I. Shklovskii.** 2000. Reentrant condensation of DNA induced by multivalent counterions. J. Chem. Phys. **112:**2562–2568.
45. **Rein, A., L. E. Henderson, and J. G. Levin.** 1998. Nucleic-acid-chaperone activity of retroviral nucleocapsid proteins: significance for viral replication. Trends Biochem. Sci. **23:**297–301.
46. **Rouzina, I., and V. A. Bloomfield.** 1996. Macroion attraction due to electrostatic correlation between screening counterions. 1. Mobile surface-adsorbed ions and diffuse ion cloud. J. Phys. Chem. **100:**9977–9989.
47. **Stewart-Maynard, K., M. Cruceanu, F. Wang, M.-N. Vo, R. J. Gorelick, M. C. Williams, I. Rouzina, and K. Musier-Forsyth.** 2008. Retroviral nucleocapsid proteins display nonequivalent levels of nucleic acid chaperone activity. J. Virol. **82:**10129–10142.
48. **Tsuchihashi, Z., and P. O. Brown.** 1994. DNA strand exchange and selective DNA annealing promoted by the human immunodeficiency virus type 1 nucleocapsid protein. J. Virol. **68:**5863–5870.
49. **Urbaneja, M. A., B. P. Kane, D. G. Johnson, R. J. Gorelick, L. E. Henderson, and J. R. Casas-Finet.** 1999. Binding properties of the human immunodeficiency virus type 1 nucleocapsid protein p7 to a model RNA: elucidation of the structural determinants for function. J. Mol. Biol. **287:**59–75.
50. **Urbaneja, M. A., M. Wu, J. R. Casas-Finet, and R. L. Karpel.** 2002. HIV-1 nucleocapsid protein as a nucleic acid chaperone: spectroscopic study of its helix-destabilizing properties, structural binding specificity, and annealing activity. J. Mol. Biol. **318:**749–764.
51. **Wang, H., K. M. Norris, and L. M. Mansky.** 2003. Involvement of the matrix and nucleocapsid domains of the bovine leukemia virus gag polyprotein precursor in viral RNA packaging. J. Virol. **77:**9431–9438.
52. **Weiss, S.** 2000. Measuring conformational dynamics of biomolecules by single molecule fluorescence spectroscopy. Nat. Struct. Biol. **7:**724–729.
53. **Williams, M. C., R. J. Gorelick, and K. Musier-Forsyth.** 2002. Specific zinc-finger architecture required for HIV-1 nucleocapsid protein's nucleic acid chaperone function. Proc. Natl. Acad. Sci. USA **99:**8614–8619.
54. **Ying, L., M. I. Wallace, S. Balasubramanian, and D. Klenerman.** 2000. Ratiometric analysis of single-molecule fluorescence resonance energy transfer using logical combinations of threshold criteria: a study of 12-mer DNA. J. Phys. Chem. B **104:**5171–5178.
55. **Zeng, Y., H.-W. Liu, C. F. Landes, Y. J. Kim, X. Ma, Y. Zhu, K. Musier-Forsyth, and P. F. Barbara.** 2007. Probing nucleation, reverse annealing, and chaperone function along the reaction path of HIV-1 single-strand transfer. Proc. Natl. Acad. Sci. USA **104:**12651–12656.
56. **Zhuang, X.** 2005. Single-molecule RNA science. Annu. Rev. Biophys. Biomol. Struct. **34:**399–414.